Potential Roles of Cornichon Family AMPA Receptor Auxiliary Protein 4 (CNIH4) in Head and Neck Squamous Cell Carcinoma

Yixue Li
Guangzhou University of Chinese Medicine
Hengrui Liu (hengrui.liu@biocomma.cn)
Biocomma Limited
Yue Han
Shenzhen Traditional Chinese Medicine Hospital

Research Article

Keywords: CNIH4, HNSC, cancer stemness, immunity

Posted Date: September 13th, 2021

DOI: https://doi.org/10.21203/rs.3.rs-845967/v1

Abstract

Background The diagnosis and prognosis of neck squamous cell carcinoma (HNSC) is a challenge for clinical HNSC management, thus, the investigation of molecular biomarkers of HNSC is urgent. We hypothesized that Cornichon Family AMPA Receptor Auxiliary Protein 4 (CNIH4) is a biomarker for HNSC.

Methods We analyzed mRNA seq data, protein staining data, and single-cell expression data of HNSC from open databases and evaluated the diagnostic and prognostic value of CNIH4, and investigated the association of CNIH4 to HNSC cancer biology and immunity.

Results CNIH4 was expressed higher and have higher copy number in HNSC compared to normal tissues. CNIH4 was associated with worse overall survival of HNSC patients. A survival nomogram was constructed. 2012 and 421genes were identified as positively and negatively associated with CNIH4 respectively, and they were enriched in “Cell cycle”, “DNA replicate”, “Cytokine–cytokine receptor interaction”, etc. CNIH4 was positively correlated with “stemness”, “cell cycle”, and “DNA repair” in single-cell data. CNIH4 was potentially associated with changes in multiple immune cell infiltration and cancer immune escape.

Conclusion CNIH4 is a diagnostic and prognostic biomarker for HNSC patients and can potentially affect the cancer stemness and tumor immune microenvironment of HNSC cells.

1. Introduction

Head and neck squamous cell carcinoma (HNSC) is one of the most common cancer types in the world. There are more than five hundred thousand new HNSC cases occur in the world, which leads to about 3 hundred thousand deaths each year [1, 2]. Conventional management for HNSC includes surgery, radiotherapy, and chemotherapy [3]. Although a number of studies have been done over the past decades, the therapy of HNSC remains largely unsatisfactory and the overall survival rate of HNSC patients over the past several years remains low. The diagnosis and prognosis of HNSC are a challenge for clinical HNSC treatment. A late diagnosis or imprecise prognosis might lead to the underestimate of cancer and if left untreated or undertreated, patients might develop lymph node metastasis that results in a much lower survival rate [4, 5]. Therefore, the investigation of molecular biomarkers of HNSC for diagnosis and prognosis is urgent.

Cornichon Family AMPA Receptor Auxiliary Protein 4 (CNIH4) is a protein-coding gene that was reported to interact with newly synthesized GPCR and regulated their export from the endoplasmic reticulum [6]. In cancer, CNIH4 was supposed to have potential effects. Studies showed that CNIH4 was found in colon cancer and promoted colon cancer metastases[7]. It was found to be one of the differential expressed genes in breast cancer [8]. CNIH4 was also proposed as one of the five genes used for signature prediction of overall survival of patients with hepatocellular carcinoma [9]. However, the clinical application of CNIH4 in many other cancer types remains largely unknown and the role of CNIH4 in cancers required further investigation.

Preliminary screening results showed that CNIH4 is a regulatory molecule for HNSC. In this study, we tested CNIH4 as a prognostic gene for HNSC patients. We also proposed that CNIH4 is a regulator for the cancer cell biology and tumor immune microenvironment in HNSC. This study provided a novel molecular marker for the improvement of clinical HNSC treatment.

2. Methods

2.1. RNA-seq and clinical data acquisition

Bioinformatic data in this study were obtained from TCGA (The Cancer Genome Atlas) in January 2020. The acquisition and the application of these data followed the guidelines and policies of TCGA.

2.2. RNA-seq data analysis

R foundation for statistical computing (2020) version 4.0.3 and ggplot (v3.3.2) was used for the analysis. The immune cell infiltration levels were analyzed using xCell algorithms. The one-class logistic regression machine learning algorithm (OCLR) [10] algorithm was used to calculate the mRNAsi for the evaluation of stemness. Potential immune checkpoint blockade (ICB) response was predicted using the Tumor Immune Dysfunction and Exclusion (TIDE) [11] algorithm.

2.3. Immunohistochemistry staining

The images of CNIH4 protein staining were downloaded from HPA (Human Protein Atlas). Antibody HPA044268 was used for the staining.

2.4. Single-cell sequencing data acquisition and analysis

The CancerSEA[12] was used to analyze the functional states and their correlation with CNIH4 expression. Single-cell datasets GSE103322[13] were analyzed. The TISCH (Tumor Immune Single-cell Hub) [14]was used to analyze the expression of CNIH4 in immune cells and malignant cells. Data sets GSE103322[13] and GSE139324[15] were analyzed. The UMAP (Dimensionality reduction via Uniform Manifold Approximation and Projection) [16] method was used to display the data. Cell-type annotations were provided by TISCH.

2.5. Statistical significance

The statistical significance was defined by a P-value of over 0.05.

3. Results

3.1. The expression of CNIH4 in HNSC

Firstly, we analyzed the CNIH4 expression in HNSC. Results showed that the expression of CNIH4 in HNSC was significantly higher than that in head and neck normal tissues (Fig. 1A1). We also found that higher grade HNSC expressed significantly higher CNIH4 than lower grade HNSC (Fig. 1A2). Samples

from male patients had significantly higher CNIH4 than those from female patients (Fig. 1A3). The pTNM IV had significantly higher CNIH4 than pTNM I, but the other comparison had no significant differences (Fig. 1A4). There was no significant difference among different pT stagings or different pN stagings (Fig. 1A5-6). Compared to the white, black patients had a slightly higher expression of CNIH4 (Fig.A7). Compared to the patients who smoke, patients who do not smoke expressed a slightly lower CNIH4 (Fig.A8). Besides, we also compared paired cancer-noncancer samples from the same patient, paired t-test showed that CNIH4 was overexpressed in cancer (Fig. 1B). Clinical information of the high (50–100%, red) and low (0–50%, blue) CNIH4 groups were listed in Table 1. To further confirm CNIH4 protein was overexpressed in HNSC compared to paired normal tissue, we compared protein staining results. Results showed that, compared to the normal oral mucosa, and HNSC tissues had a higher staining intensity of CNIH4 (Fig. 2). Thus, CNIH4 was a diagnostic marker of HNSC. In addition, to investigate the reason for overexpression of CNIH4 in HNSC, we compared the copy number of CNIH4 in HNSC and normal tissues in 27 data sets. The overall statistical analysis revealed that the copy number of CNIH4 in HNSC was significantly higher than that in normal tissues. Specifically, the copy number of CNIH4 in HNSC was significantly higher than normal tissues in 20 of the 27 data sets (Fig. 3). Therefore, we suggested that the overexpression of CNIH4 in HNSC resulted from the higher gene copy number of CNIH4 in HNSC.

Table 1
Distribution of HNSC patients with different clinicopathological variables in CNIH4 high and low groups.

Term	AIMP1 high	AIMP1 low	P-value
Alive	122	162	
Dead	129	89	0
Mean (SD)	61.9 (11)	60.2 (12.7)	
Median [MIN,MAX]	61 [26,87]	60 [19,90]	0.103
FEMALE	61	73	
MALE	190	178	0.19
ASIAN	3	7	
BLACK	31	16	
WHITE	206	222	0.074
T1	16	18	
T2	65	79	
T3	65	68	
T4	16	9	
T4a	78	74	
T4b	2	1	
TX	9	2	0.21
N0	121	120	
N1	38	43	
N2	9	10	
N2a	10	8	
N2b	35	41	
N2c	21	20	
N3	6	1	
NX	11	8	0. 644
M0	234	243	
M1	3	2	

Term	AIMP1 high	AIMP1 low	P-value
MX	14	6	0. 168
I	8	17	
II	39	42	
III	42	48	
IVA	151	139	
IVB	10	3	
IVC	1	2	0.381
G1	19	43	
G2	146	154	
G3	73	46	
GX	11	5	
G4		2	0
Metastasis	11	8	
Primary	6	3	
Recurrence	24	15	0.904
Non-smoking	44	67	
Smoking	203	178	0.015
Non-radiation	29	33	
Radiation	66	55	0.401
Neoadjuvant	7	3	
No neoadjuvant	244	248	0.338
Chemotherapy	83	76	

3.2. Survival Prognostic analysis of CNIH4 gene in HNSC.

To evaluate the prognostic power of CNIH4 for HNSC patients, we analyzed the association of CNIH4 expression and the overall survival of HNSC patients. We conducted a Kaplan-Meier survival analysis and log-rank test to compare the survival of the high (50–100%, red) and low (0–50%, blue) CNIH4 groups. The HR for the high CNIH4 group was 1.5 (95%IC = 1.152–1.983) and the median time for high and low CNIH4 groups were 3 and 5.2 respectively (Fig. 4A). Therefore, we suggested that CNIH4 was a potential impact factor for the overall survival of HNSC. To apply the CNIH4 expression to the clinical prognosis of

HNSC, we constructed a survival nomogram. Variables CNIH4 expression, age, gender, grade, and race were analyzed. Univariate Cox regression analysis results showed that, among these five variables, only CNIH4 expression and age were significantly associated with survival (Fig. 4B). Multivariate Cox regression showed that CNIH4 expression and age were independent factors for HNSC patient survival (Fig. 4C). Therefore, based on the Cox regression results, a nomogram including variables CNIH4 expression and age was constructed for the prediction of 1-, 2-, 3-, 5- year survival for HNSC patients. The C-index of the nomogram was 0.602 (Fig. 4D). The prediction results of the nomogram calibration curves were consistent with all patients' observation results (Fig. 4E). These analyses demonstrated the clinical value of CNIH4 for HNSC prognosis.

3.3. CNIH4 associated genes enrichment analysis.

To explore the potential mechanisms involved in the effect of the CNIH4 gene on HNSC, we identified differentially expressed genes (DEGs) between CNIH4 high (75–100%) and low (0–25%) groups. We set cutoff values of 1.5 and 0.01 for fold change and p-value respectively. Results showed that 2012 and 421 genes were identified as DEGs positively and negatively associated with CNIH4 in HNSC respectively (Fig. 5AB). These genes were further enriched in GO terminologies and KEGG pathways. Results of KEGG enrichment showed that genes positively associated with CNIH4 were most enriched in “Cell cycle”, while genes negatively associated with CNIH4 were most enriched in “Cytokine − cytokine receptor interaction”. In terms of GO enrichment, genes positively associated with CNIH4 were highly enriched in “organelle fission”, “nuclear division”, “mitotic nuclear division”, “chromosome segregation”, and “DNA replication”, while genes negatively associated with CNIH4 were highly enriched in “epidermis development”, “skin development”, “epidermal cell differentiation”, “keratinization”, and “keratinocyte differentiation” (Fig. 5C). Other less enriched terms included immune-associated terms, such as “T cell activity”. Because these genes were enriched in multiple terms that were associated with cancer stemness and immune cells, these results inferred that CNIH4 might play a role in cancer stemness and regulation of immunity in HNSC.

3.4. CNIH4 was associated with stemness of HNSC

To further explore the potential role of CNIH4 in HNSC, we investigated a single-cell data set of HNSC. We analyzed the correlation of CNIH4 expression and cancer functional state scores of 2150 single HNSC cells and identified 12 functional states that significantly correlated with CNIH4 ($p < 0.05$). Results showed that CNIH4 was positively correlated with stemness, cell cycle, DNA repair, invasion, and proliferation with coefficients of 0.26, 0.23, 0.13, 0.06, and 0.05 respectively. On the other hand, CNIH4 was negatively correlated with angiogenesis, quiescence, metastasis, hypoxia, inflammation, DNAdamage, and differentiation with coefficients of -0.16, -0.16, -0.10, -0.10, -0.08, -0.07, and − 0.06 (Fig. 6A). Detailed data were shown in Fig. 6B. As the correlations of stemness and cell cycle were striking, we further demonstrate the association of CNIH4 and cancer stemness. We applied OCLR to compared the stemness of CNIH4 high (75–100%) and low (0–25%) groups. Results showed that the CNIH4 high group had significantly higher stemness than that of the low groups, indicating that CNIH4

might upregulate stemness of HNSC. These results were consistent with the enrichment results that CNIH4 was associated with “cell cycle” and “DNA replicate”.

3.5. CNIH4 was associated with immunity regulation of HNSC

To study the potential role of CNIH4 in the immunity of HNSC, we first analyzed the distribution of CNIH4 in different cell fractions in HNSC. Single-cell seq data sets HNSC_GSE103322 and HNSC_GSE139324 were analyzed. Results showed that HNSC malignant cells expressed much higher CNIH4 than immune cells (Fig. 7). Therefore, we suggested that the expression level of CNIH4 in HNSC samples was mainly dependent on the expression of CNIH4 in tumor cells. Furthermore, we calculated the immune cell infiltration score of TCGA data using the xCell algorithms. We compared immune cell infiltration levels between CNIH4 high (75–100%) and low (0–25%) groups. In detail, compared to the CNIH4 low group, the CNIH4 high group was only significantly higher in the levels of Common lymphoid progenitor and T cell CD4 + Th2. However, CNIH4 high group was significantly lower at levels of T cell CD4 + central memory, Endothelial cell, Myeloid dendritic cell activated, Myeloid dendritic cell, Plasmacytoid dendritic cell, T cell CD8+, T cell CD8 + central memory, B cell plasma, B cell, B cell memory, T cell CD4 + naïve, Class − switched memory B cell, Monocyte, Neutrophil, Mast cell, and T cell CD4 + effector memory. These results suggested that CNIH4 was negatively associated with infiltration levels of most immune cells and might negatively regulate immune and stroma in HNSC. Apart from that, we analyzed the correlation of CNIH4 and four immune checkpoints, including CTLA4, LAG3, PDCD1, and TIGIT. Results showed that CNIH4 expression was negatively correlated with CTLA4, LAG3, PDCD1, and TIGIT expression (Fig. 8-B). To further explore the value of CNIH4 for clinical immune therapy, we compared ICB respond of CNIH4 low (0–25%) and high (75–100%) groups. Potential ICB response was predicted using the TIDE algorithm. Results showed that the CNIH4 low group had a significantly higher TIDE score than the CNIH4 high group (Fig. 8 bottom). The calculation predicted that only 28 out of 98 (22.22%) HNSC patients responded to ICB treatment in the low CNIH4 group, while 84 out of 126 (66.67%) respond to ICB treatment in the high CNIH4 group (Fig. 8 top).

4. Discussion

This is the first study reported that CNIH4 was overexpressed in HNSC compared to normal squamous epithelial tissues. We also revealed that this overexpression was, at least partly, resulted from the increased gene copy number in HNSC, but other factors such as transcriptional factor or methylation can also contribute to the overexpression of CNIH4 in cancer. We also found that the expression of CNIH4 is associated with higher grade HNSC. Thus, our data supported that CNIH4 was a potential diagnostic and prognostic biomolecule in HNSC. A previous study reported that CNIH4 was upregulated in colon cancer [7], which was consistent with our initial proposal that cancer tissues might express higher CNIH4 than their corresponding normal tissues. Thus, we believe that CNIH4 has similar expression patterns and

effects in different tumor types. However, to date, the expression pattern of CNIH4 in most other cancer types has not been studied.

One of the most striking findings of this study was that CNIH4 expression potentially affects the overall survival of HNSC patients. The Cox regression analysis indicated that CNIH4 was a risky factor for HNSC patients and it was independent of patients' age, gender, grade, and race. Although a previous study suggested CNIH4 was valuable in the prognosis of hepatocellular carcinoma patients [9], the clinical prognostic value of CNIH4 for HNSC patients has never been reported previously. In this study, we constructed a nomogram to demonstrate the clinical value of CNIH4 for HNSC prognosis. Hence, our analysis provided a potential biomarker for clinical HNSC diagnosis and prognosis.

Although our results showed that CNIH4 was associated with worse survivals of HNSC patients and CNIH4 expression might increase during the development of HNSC, it was not clear what role CNIH4 played in HNSC. Previously, a study reported that the protein secretion modulator TMED9 drives CNIH4 signaling to inhibit TMED3-WNT-TCF, thereby promoted the migration of colon cancer [7]. In the present study, the enrichment results showed that CNIH4 was positively associated with some stemness-related terms, such as "cell cycle" and "DNA replication". Cancer proliferation is largely dependent on the cancer stem cells [17]. The OCLR score also demonstrated that high CNIH4 might result in a higher stemness of HNSC. In addition, in the single-cell analysis, stemness and cell cycle and DNA replicate were the three most CNIH4-correlated states with considerable large coefficients. These single-cell data further supported CNIH4 as a biomarker of cancer stemness in HNSC and accounted for the association of CNIH4 and more severe HNSC. Further functional validation of the stemness of CNIH4 in HNSC cells is required in the future.

Another interesting finding in the enrichment study was that CNIH4 might be involved in immunity in HNSC. These results raised our interest in the effect of CNIH4 in tumor immune therapy. Immunotherapies such as immune checkpoint therapy (ICT), tumor vaccines, immune adaptive therapy, and immunomodulators have been applied in many cancers [18]. Tumor immune single-cell data showed that HNSC tumor cells expressed a much higher level of CNIH4 than immune cells. These results indicated that a higher level of CNIH4 in HNSC samples of TCGA should result from higher levels of CNIH4 in tumor cells. The immune infiltration analysis revealed that CNIH4 was negatively associated with most of the immune cell infiltration levels. The only two positive associated immune cell types were common lymphoid progenitor and T cell CD4 + Th2. The response of immune therapy is supposed to be dependent on the immune cell infiltration level and the expression of immune checkpoint molecules. Immune checkpoints have modulatory effects on immunity [19]. By these immune checkpoint molecules, cancer cells can escape from the immunity. CNIH4 expression was negatively correlated with immune checkpoint molecules CTLA4, LAG3, PDCD1, and TIGIT, inferring that CNIH4 might promote the immune escape. On the other hand, we also analyzed the TIDE score, which evaluating immune escape using a set of marker genes. TIDE score indicated the dysfunction of tumor-infiltrating cytotoxic T lymphocytes (CTL) and the exclusion of CTL by immunosuppressive factors [11]. Patients with a high TIDE score have worse response to the ICB. Our analysis showed that CNIH4 was associated with a TIDE score, indicating

that high CNIH4 HNSC might be easier to escape from cancer immunity and not respond to ICB. These results suggested that patients with higher CNIH4 were more likely to respond to immunotherapy. Therefore, we proposed that CNIH4 was a sign of ICB-responsive HNSC.

In conclusion, this study demonstrated that CNIH4 is a diagnostic and prognostic biomarker for HNSC patients and can potentially affect the cancer stemness and tumor immune microenvironment of HNSC cells.

Declarations

Availability of data and materials

The source of the raw data was provided in the paper and the raw analysis data of this study are provided by the corresponding author with a reasonable request.

Competing interests

The authors claimed that there is no conflict of interest.

Consent for publication

All the author consent for this publication.

Funding

This study received funding from Shenzhen Traditional Chinese Medicine Hospital.

Ethical approval

Not applicable.

Authors' contributions

Hengrui Liu contributed to the design of the study. Yixue Li and Yue Han contributed to the data acquisition, data analysis, and Yixue Li and Hengrui Liu composed the manuscript. Yue Han provided clinical academic advice in the study. Hengrui Liu supervised the project. All authors had given final approval of the version to be published.

Author information

The corresponding author of this study, Hengrui Liu, is a Principal Investigator in Biocomma Limited.

References

1. Siegel RL, Miller KD, Jemal A. Cancer statistics, 2019. CA: a cancer journal for clinicians. 2019; 69: 7–34.
2. Wingo PA, Cardinez CJ, Landis SH, Greenlee RT, Ries LA, Anderson RN, et al. Long-term trends in cancer mortality in the United States, 1930–1998. Cancer. 2003; 97: 3133–275.
3. Miller KD, Nogueira L, Mariotto AB, Rowland JH, Yabroff KR, Alfano CM, et al. Cancer treatment and survivorship statistics, 2019. CA: a cancer journal for clinicians. 2019; 69: 363–85.
4. Duprez F, Berwouts D, De Neve W, Bonte K, Boterberg T, Deron P, et al. Distant metastases in head and neck cancer. Head & neck. 2017; 39: 1733–43.
5. Chiesa-Estomba CM, Lechien JR, Ayad T, Calvo-Henriquez C, Gonzalez-Garcia JA, Sistiaga-Suarez JA, et al. Clinical and histopathological risk factors for distant metastasis in head and neck cancer patients. Acta Otorhinolaryngol Ital. 2021; 41: 6–17.
6. Sauvageau E, Rochdi MD, Oueslati M, Hamdan FF, Percherancier Y, Simpson JC, et al. CNIH4 interacts with newly synthesized GPCR and controls their export from the endoplasmic reticulum. Traffic (Copenhagen, Denmark). 2014; 15: 383–400.
7. Mishra S, Bernal C, Silvano M, Anand S, Ruiz IAA. The protein secretion modulator TMED9 drives CNIH4/TGFα/GLI signaling opposing TMED3-WNT-TCF to promote colon cancer metastases. Oncogene. 2019; 38: 5817–37.
8. Varisli L. Gene Expression Signatures of Ductal Breast Carcinoma Shows Differentially Expression of Cell Cycle, Proliferation and Apoptosis Related Genes. World Journal of Research and Review. 3: 262904.
9. Wang Z, Pan L, Guo D, Luo X, Tang J, Yang W, et al. A novel five-gene signature predicts overall survival of patients with hepatocellular carcinoma. Cancer Med. 2021; 10: 3808–21.
10. Malta TM, Sokolov A, Gentles AJ, Burzykowski T, Poisson L, Weinstein JN, et al. Machine Learning Identifies Stemness Features Associated with Oncogenic Dedifferentiation. Cell. 2018; 173: 338 – 54.e15.
11. Jiang P, Gu S, Pan D, Fu J, Sahu A, Hu X, et al. Signatures of T cell dysfunction and exclusion predict cancer immunotherapy response. Nature medicine. 2018; 24: 1550–8.
12. Yuan H, Yan M, Zhang G, Liu W, Deng C, Liao G, et al. CancerSEA: a cancer single-cell state atlas. Nucleic Acids Res. 2019; 47: D900-d8.
13. Puram SV, Tirosh I, Parikh AS, Patel AP, Yizhak K, Gillespie S, et al. Single-Cell Transcriptomic Analysis of Primary and Metastatic Tumor Ecosystems in Head and Neck Cancer. Cell. 2017; 171: 1611-24.e24.
14. Sun D, Wang J, Han Y, Dong X, Ge J, Zheng R, et al. TISCH: a comprehensive web resource enabling interactive single-cell transcriptome visualization of tumor microenvironment. Nucleic Acids Res. 2021; 49: D1420-d30.
15. Cillo AR, Kürten CHL, Tabib T, Qi Z, Onkar S, Wang T, et al. Immune Landscape of Viral- and Carcinogen-Driven Head and Neck Cancer. Immunity. 2020; 52: 183 – 99.e9.

16. McInnes L, Healy J, Melville J. Umap: Uniform manifold approximation and projection for dimension reduction. arXiv preprint arXiv:180203426. 2018.
17. Liu H. A Prospective for the Potential Effect of Local Anesthetics on Stem-Like Cells in Colon Cancer. Biomedical Journal of Scientific & Technical Research. 2020; 25: 18927–30.
18. Chen X, Lan H, He D, Wang Z, Xu R, Yuan J, et al. Analysis of Autophagy-Related Signatures Identified Two Distinct Subtypes for Evaluating the Tumor Immune Microenvironment and Predicting Prognosis in Ovarian Cancer. Frontiers in oncology. 2021; 11: 616133-.
19. Li B, Chan HL, Chen P. Immune Checkpoint Inhibitors: Basics and Challenges. Curr Med Chem. 2019; 26: 3009–25.

Figures

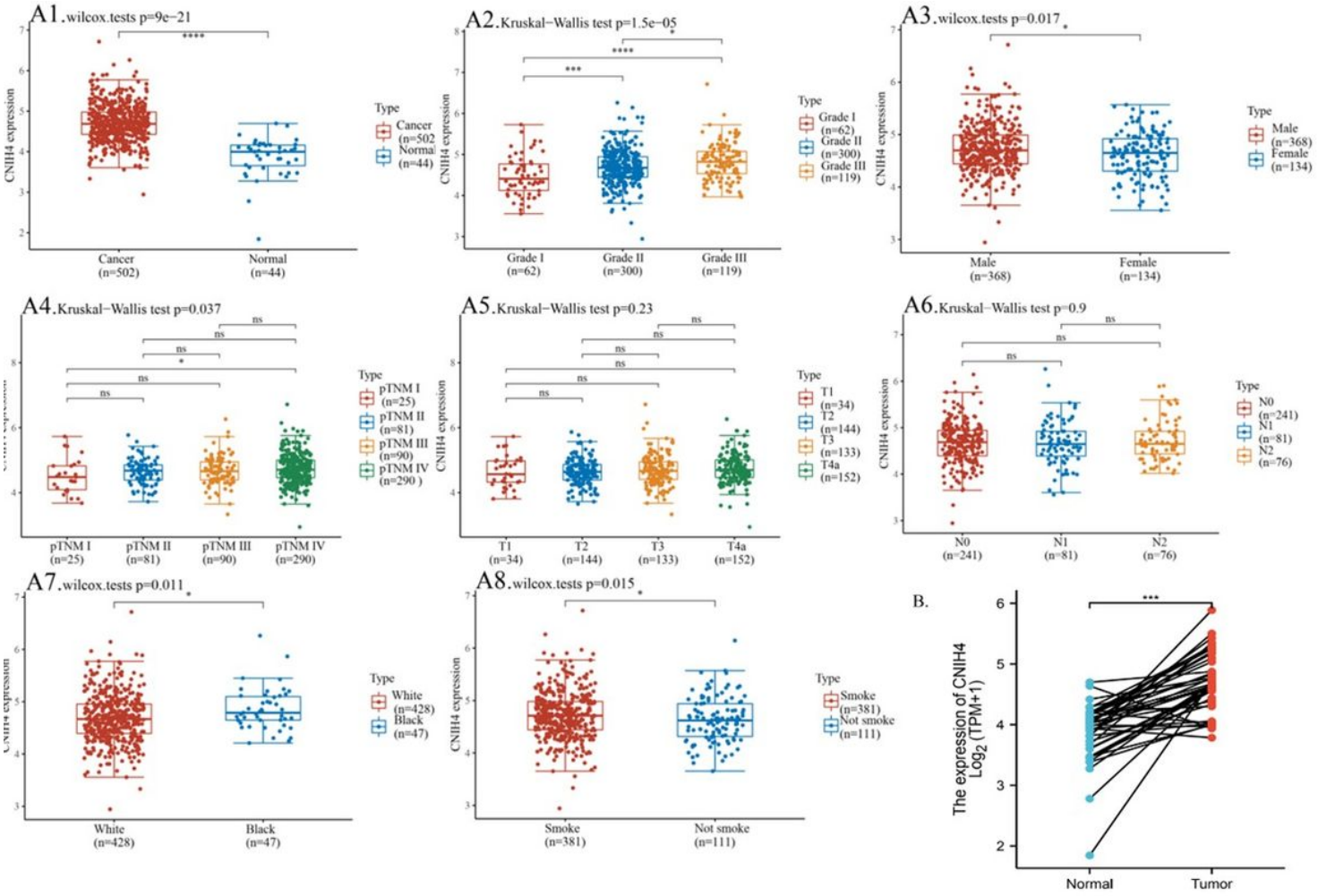

Figure 1

The expression of CNIH4 in HNSC. A1. The expression of CNIH4 in HNSC and normal head and neck tissues. TCGA and GETx data were plotted. A2-8. CNIH4 expression levels in HNSC of different clinicopathological groups. B. The expression of CNIH4 in HNSC and normal head and neck tissues.

TCGA paired data were plotted, cancer and non-cancer samples were linked. Paired t-test was used to analyze the difference.

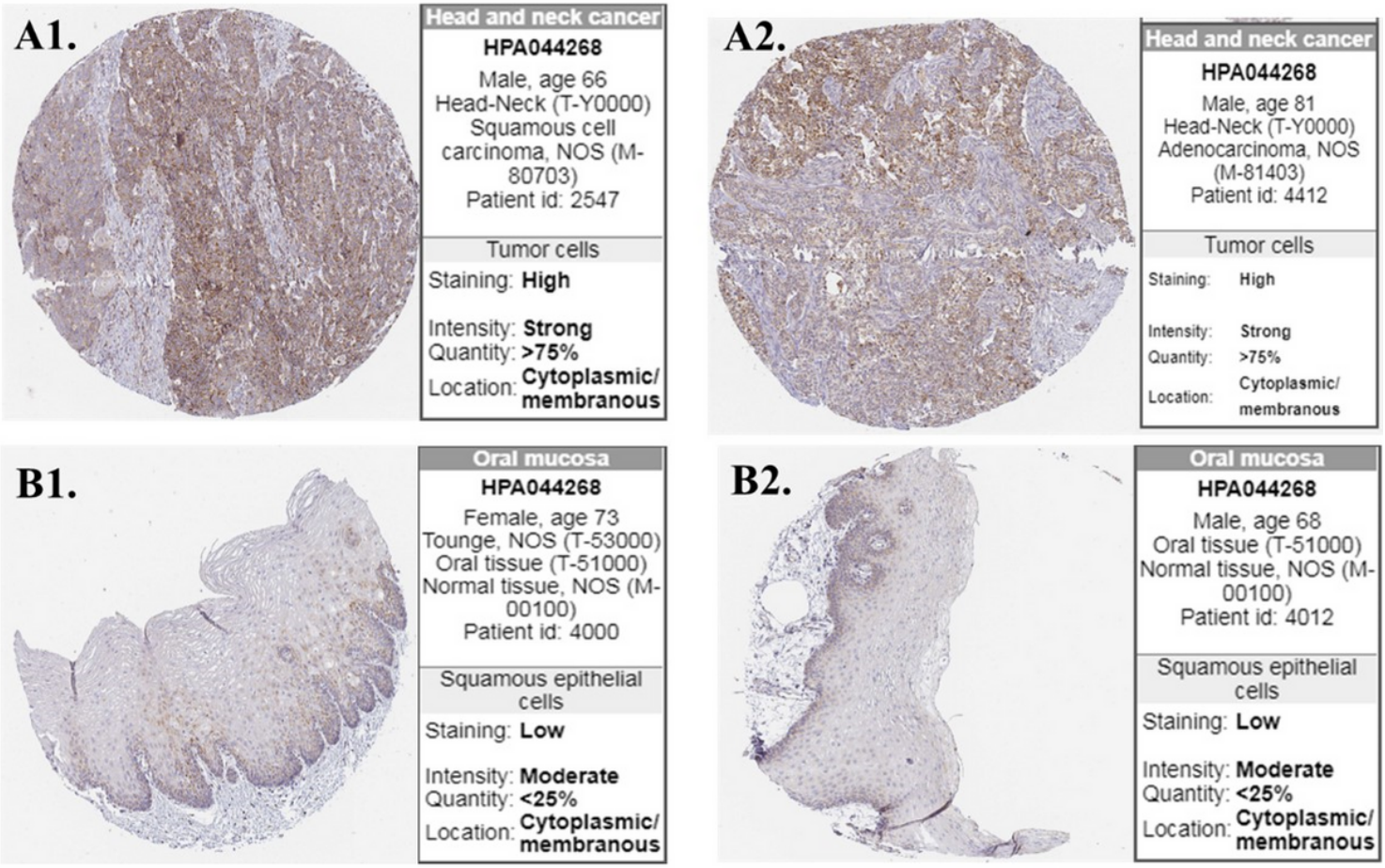

Figure 2

Protein staining images of CNIH4. The images were downloaded from the Human Protein Atlas. Antibody HPA044268 was used to stain CNIH4. A. HNSC tissues, B. Normal oral mucosa epithelial tissues.

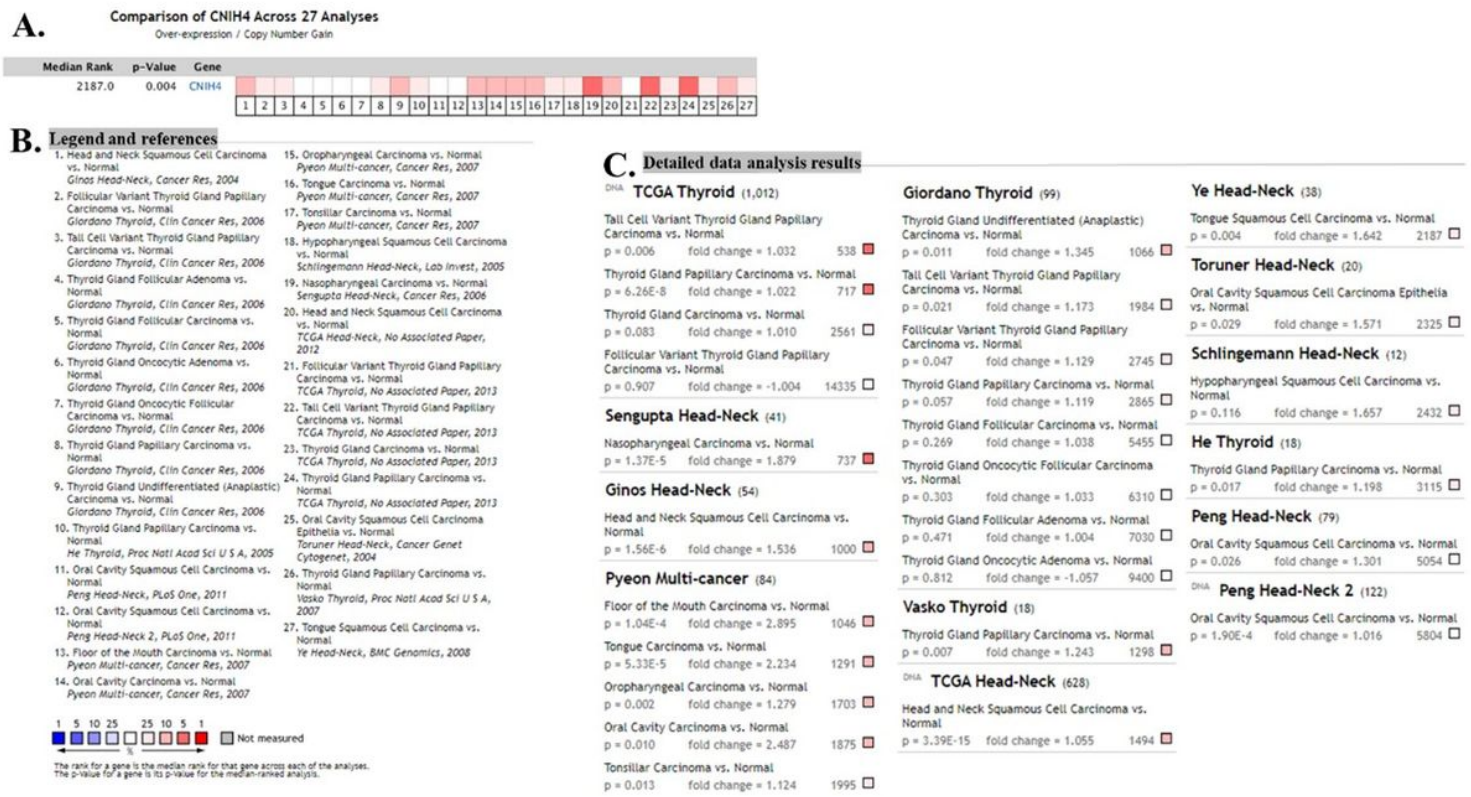

Figure 3

DNA copy number of CNIH4 in HNSC. Multiple data sets were accessed and analyzed using the Oncomine. A. Heatmap and overall copy number difference analysis between HNSC and normal tissues. B. Figure legend and references for A. C. Detailed data analysis results of data sets respectively. The p-value, fold change, and sample sizes were shown.

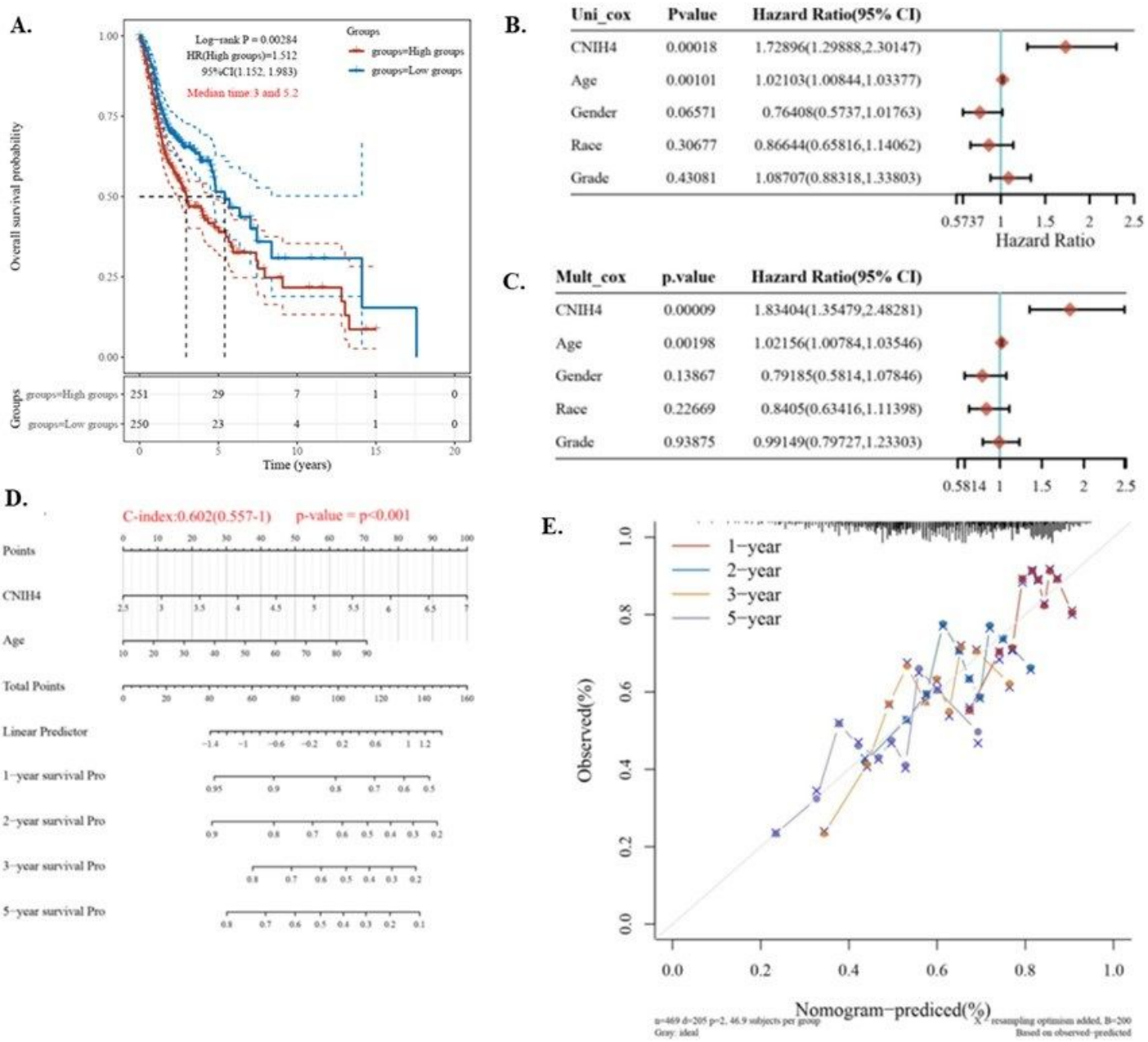

Figure 4

The prediction power of the CNIH4 gene for the survival of HNSC patients. Log-rank analysis was used to evaluate the survival association of CNIH4. Cox regression was used to evaluate the predictive value of variables CNIH4 expression, age, gender (male or female), race (white or others), and grade. A. Kaplan-Meier plot of the high (50-100%, red) and low (0-50%, blue) CNIH4 groups. Log-rank analysis results were shown. B. Univariate Cox regression analysis of overall survival of HNSC. C. Multivariate Cox regression analysis of overall survival of HNSC. D. Nomogram for the prediction of 1-, 2-, 3-, and 5-year survival. the

C-index and non-zero p-value were shown. E. Calibration plots of the nomogram for estimation of overall survival at 1-, 2, -3-, 5- year.

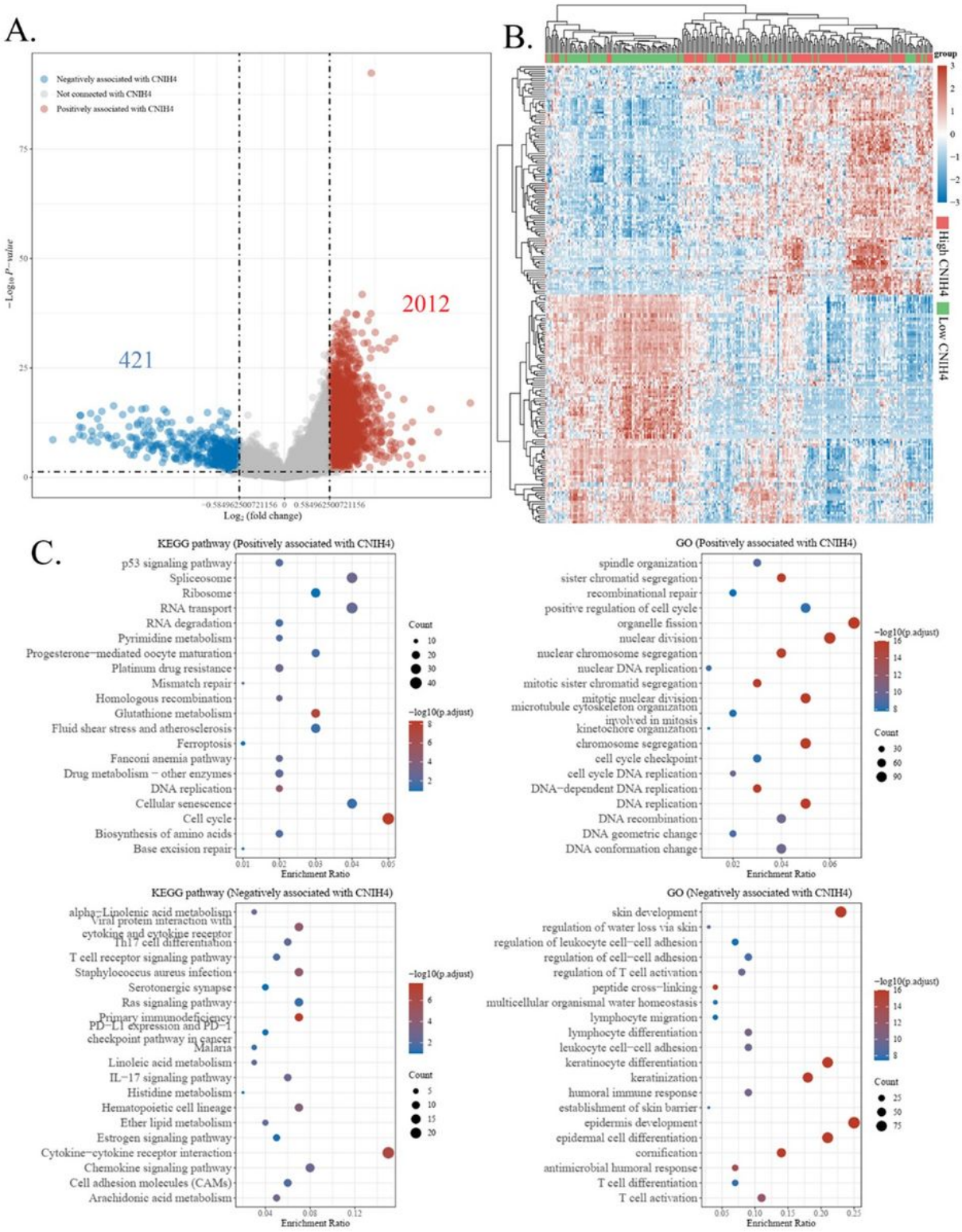

Figure 5

CNIH4 associated genes enrichment analysis. Differential gene analysis in HNSC CNIH4 high (75-100%) and low (0-25%) groups with the fold-change cutoff of >1.5 and P-value cutoff of <0.01. A. Volcano plots of CNIH4 associated genes. The red spots in the plot represent the gene positively associated with CNIH4

and the blue spots represent the gene negatively associated with CNIH4. B. Heat map and hierarchical clustering analysis of CNIH4 associated genes. C. The GO and the KEGG enrichment analysis of CNIH4 associated genes.

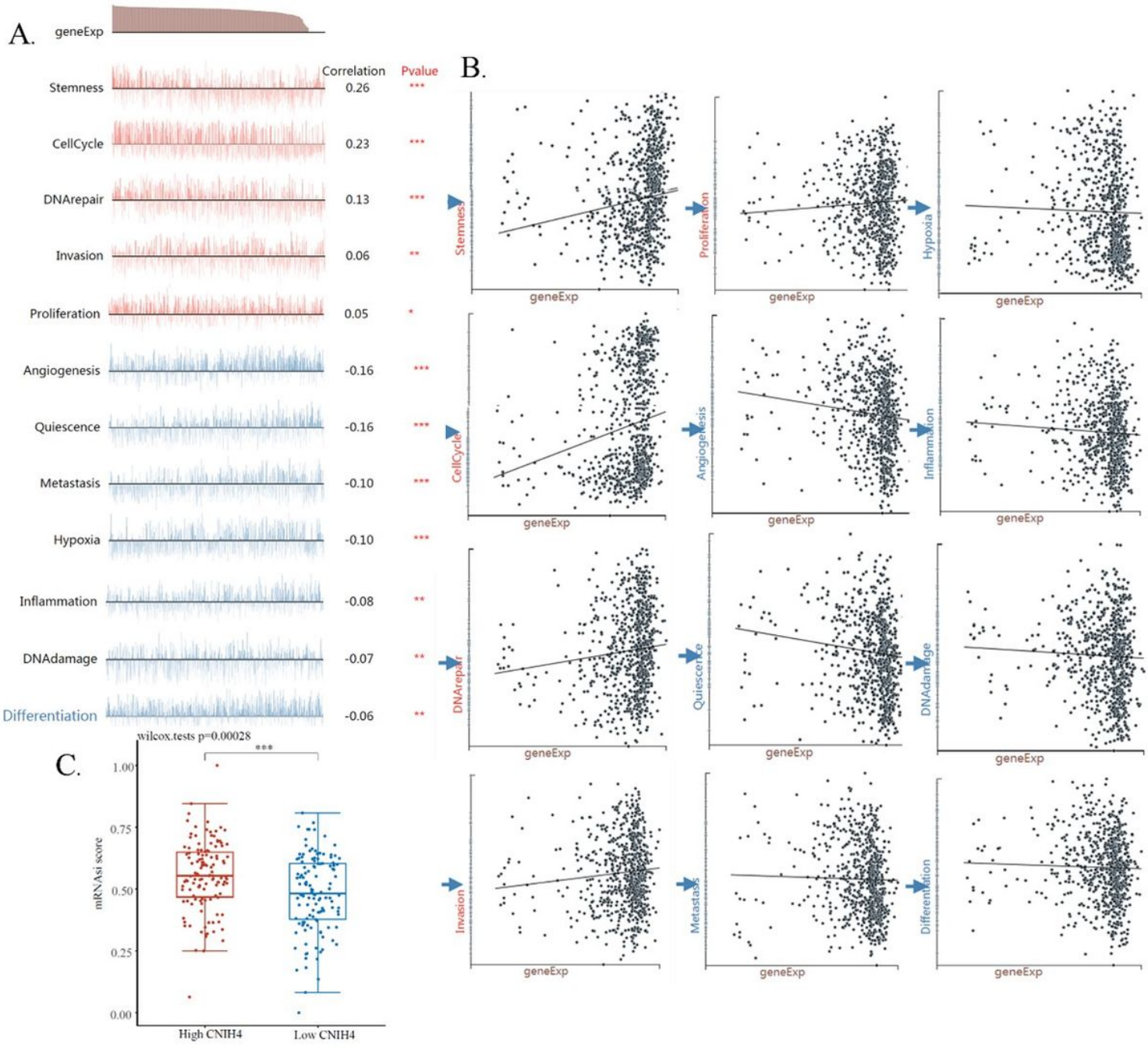

Figure 6

Association of CNIH4 and stemness. A. Correlations between CNIH4 expression and functional states in HNSC single-cell datasets. The GSE103322 data (n=2105) were accessed and analyzed using the CancerSEA. The correlation factors and significance were presented. *** p<0.001; ** p<0.01; * p<0.05. B. Scatter plot of the significant correlations between CNIH4 expression and functional states. Grey points were not considered to compute the correlations. C. The distribution of OCLR scores in TCGA HNSC

CNIH4 high (75-100%) and low (0-25%) groups. OCLR algorithm was used to calculate the mRNAsi for the evaluation of stemness.

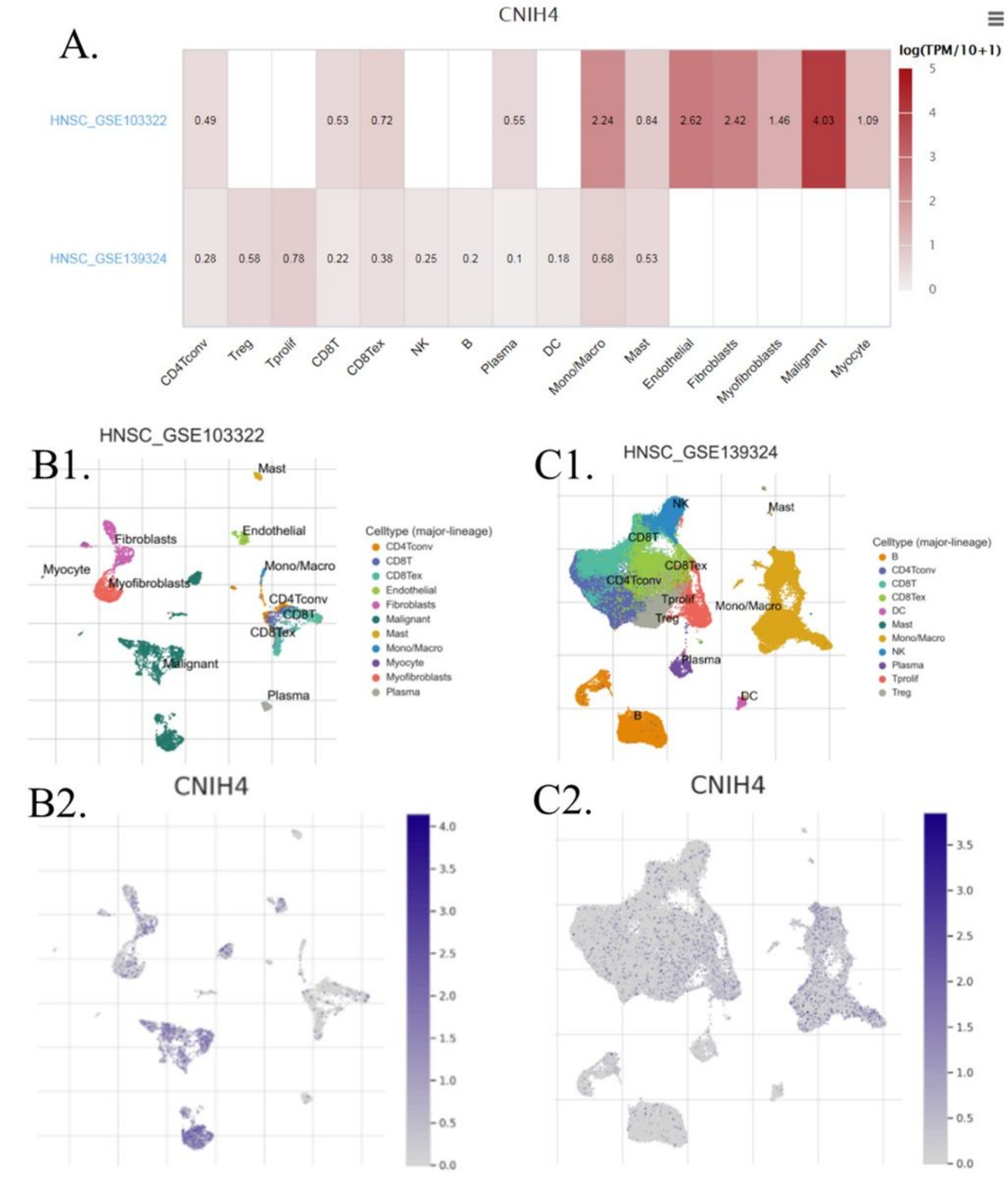

Figure 7

The expression of CNIH4 in different types of cells in HNSC samples. The data were accessed and analyzed using TISCH. A. Average expression of genes CNIH4 different cell-types across datasets

(Heatmap). B1-2. HNSC_GSE103322. C1-2. HNSC_GSE139324. The gene expression level was displayed using UMAP.

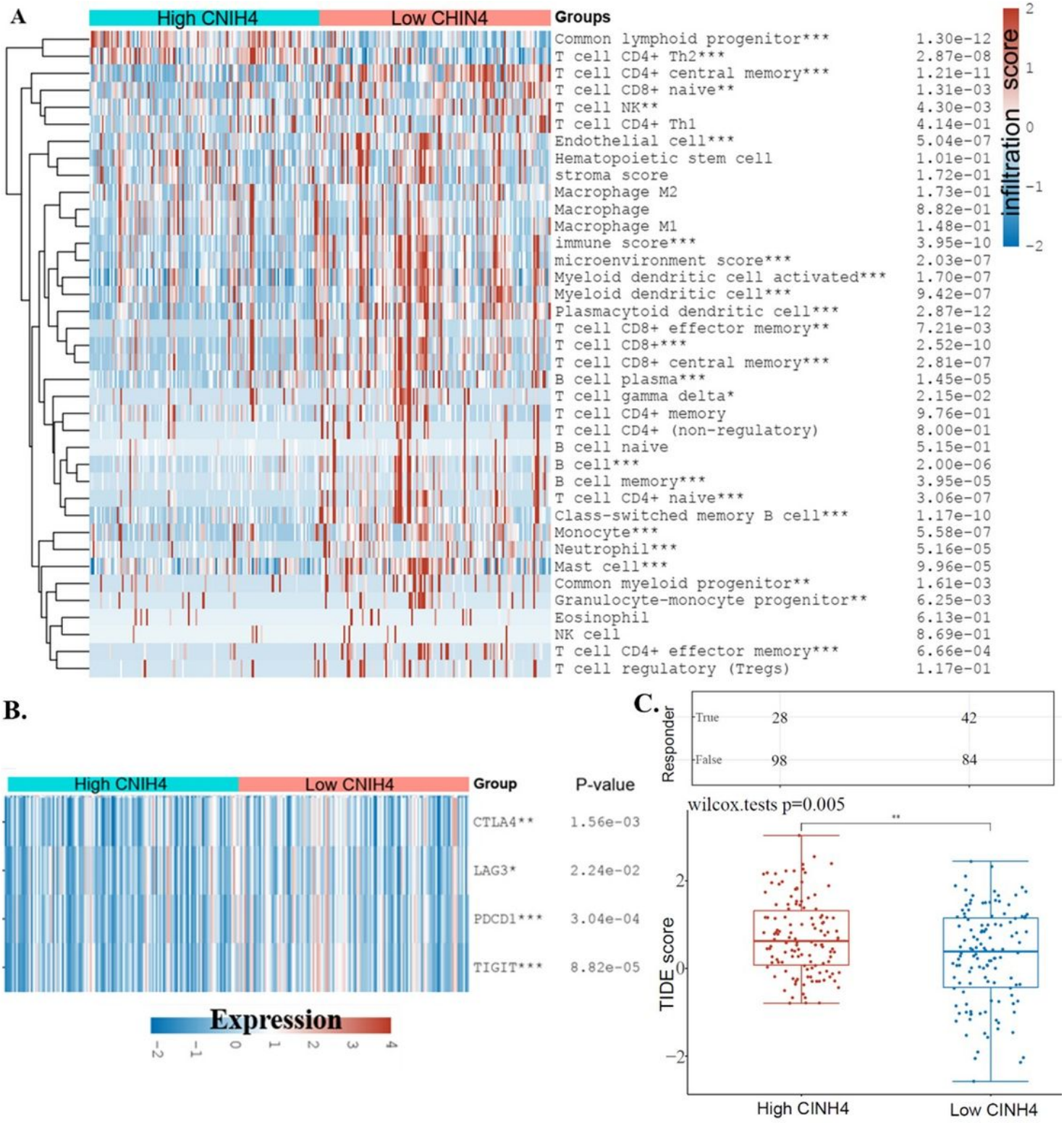

Figure 8

The effect of CNIH4 on the immunity in HNSC. A. Comparison of immune cell infiltration levels of high CNIH4 (75-100%) vs. low CNIH4 (0-25%) groups. The xCell algorism was used to calculate the levels of immune cell infiltration. The significance was calculated using the Wilcox test. *p < 0.05, **p < 0.01, ***p <

0.001. B. The expression of four immune checkpoint genes in high CNIH4 (75-100%) and low CNIH4 (0-25%) groups. C. Immune checkpoint blockade (ICB) analysis. CNIH4 low (0-25%) and high (75-100%) groups were compared. Potential ICB response was predicted using the TIDE algorithm.